Basalts from Rose Atoll, American Samoa

Article *in* Records of the Australian Museum · August 2003

DOI: 10.3853/j.0067-1975.55.2003.1380

3 authors, including:

Frederick. Lin . Sutherland
Australian Museum
139 PUBLICATIONS **2,065** CITATIONS

SEE PROFILE

Records of the Australian Museum (2003) Vol. 55: 141–152. ISSN 0067-1975

Basalts from Rose Atoll, American Samoa

K.A. RODGERS[1], F.L. SUTHERLAND[2]* AND P.W.O. HOSKIN[3]

[1] Research Associate, Australian Museum, 6 College Street, Sydney NSW 2010, Australia

[2] Geodiversity Research Centre,
Australian Museum, 6 College Street, Sydney NSW 2010, Australia
lins@austmus.gov.au

[3] Institut für Mineralogie, Petrologie und Geochemie,
Albert-Ludwigs Universität Freiburg, Albertstrasse 23b, D-79104 Freiburg in Breisgau, Germany

ABSTRACT. Three specimens of lava float collected in 1939 from Rose Atoll consist of three distinct basalt types: holocrystalline olivine tholeiite, coarse vesicular picrite basalt and olivine-poor transitional basalt; the tholeiite contains coarser, late-stage segregations with a glassy, silicic mesostasis. In mineralogy and chemistry these basalts most closely resemble Ta'u Group lavas of the neighbouring Manu'a Islands. Differences exist that do not suggest their transport to Rose Atoll, even though no in situ basalts are known there. Incompatible primitive mantle-normalized trace element plots show strong depletion in K and Sr and enrichment in U, Pb and La. In Ba/Nb versus La/Nb plots Rose basalts lie between normal mid-ocean ridge basalt (N-MORB) and low $^{87}Sr/^{86}Sr$ oceanic island basalt (OIB) fields. They lie outside many plume-related OIB fields, including plume-related Samoan basalts. Trace element ratios for the Rose samples show little correspondence with end member MORBs and OIBs. This, and temporal and geographic plume reconstructions, indicate that the Rose basalts are derived from melting of unusual or mixed lithospheric sources. They seem unrelated to the main phases of Samoan plume activity, now located at Vailulu'u Seamount.

RODGERS, K.A., F.L. SUTHERLAND & P.W.O. HOSKIN, 2003. Basalts from Rose Atoll, American Samoa. *Records of the Australian Museum* 55(2): 141–152.

Basalts found on Rose Atoll, American Samoa, present an enigma. To date petrologists have overlooked the seemingly conflicting reports of infrequent expeditions to the island (Sachet, 1954, 1955; Keating, 1992; Rodgers *et al*., 1993). Yet, given the geographic position at the eastern end of the Samoan chain, the age and nature of any basalts there are important in constraining the tectono-volcanic evolution of this chain. Only one brief description of a thin section of Rose basalt exists (Sachet, 1954). Here we present petrographic descriptions and chemical data for three samples from Rose held by the Smithsonian Institution (NMNH no. 102227) —the only known captive samples. From this we offer an assessment of their possible provenance.

Rose Atoll

Rose Atoll (14°32'S 168°08'W) lies 240 km ESE of Pago Pago at the eastern end of the Samoan Islands, part of a 1700 km long chain of seamounts, shallow banks and submerged atolls (Fig. 1). These volcanic features show an orientation consistent with their potential generation by

* author for correspondence

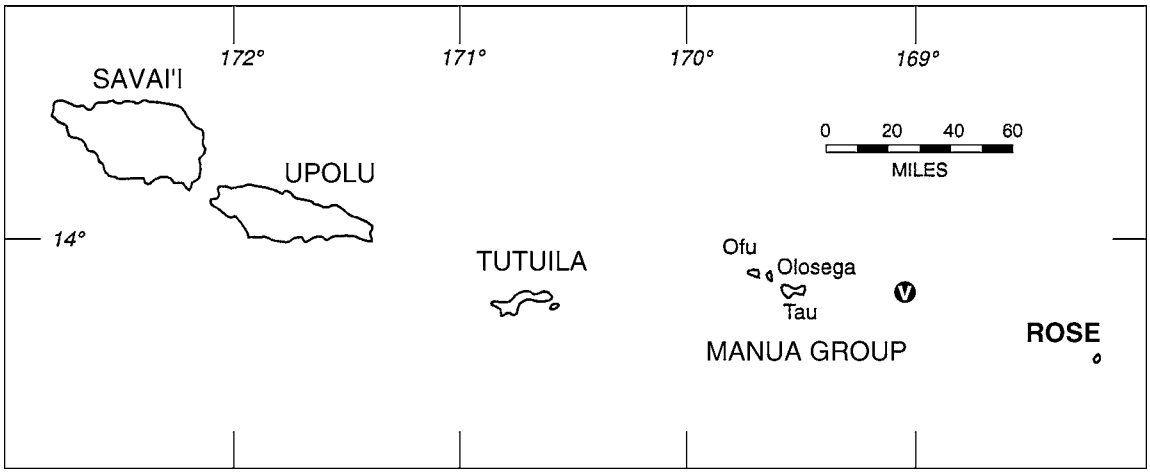

Fig. 1. Location map of Rose Atoll within the Samoan Island Chain. Vailulu'u submarine volcano (V) is located at 14°13'S 169°04'W.

Pacific plate motion over a fixed thermal anomaly (e.g., Natland, 1980; Menard, 1986). Island size and proportion covered with Quaternary lava flows increases to the west, in contrast to the Hawaiian, Society and Marquesas lineaments. There, submerged volcanic mounds, both drowned and capped by atoll reefs, occur at their western end. In contrast to mature submerged atolls and banks of the Samoan chain, Rose lacks wide offshore banks. It appears very young. The fetch of the lagoon is only 2 km and with the fringing reef and lagoon together covering just 640 ha, the atoll is among the smallest in the world. No in situ basalt is known on Rose Island.

The United States Exploring Expedition of 1839 reported loose boulders of vesicular lava ranging from 20 to 200 pounds in weight, scattered on the reef flat and in the lagoon (Couthouy, 1842; Wilkes, 1844; Dana, 1849, 1851; Pickering, 1876). In the absence of in situ basalt, Dana (1849, p. 309) suggested these boulders may have "been carried there by floating logs, or as ballast of some canoe." In 1920, Mayor (1921, 1924) looked for but failed to find volcanic rocks. He and Setchell (1924) dismissed the earlier reports as incorrect identifications of dark coloured, weathered limestone that abounds on the reef. However, in June 1939, Schultz (1940) sampled from a dozen boulders of lava lying on the reef flat and Dr Gilbert Corwin of the Smithsonian Institution subsequently confirmed these as olivine basalt (Sachet, 1954).

In evaluating these accounts, Keating (1992) cites a personal report from Dr Balzas, a herpetologist, that the only volcanic rocks he observed during several visits to Rose in the 1980s were float he attributed to transport by Samoans for use in traditional cooking. While this interpretation could account for some smaller boulders, it is implausible for larger masses, and fails to account for their reported number, variations in the observations and scattered distribution across the fringing reef and within the lagoon. These all strongly suggest basalt is being released from adjacent underwater sources, perhaps during large storms.

Material and methods

The rocks described here are those collected by Schultz and identified by Corwin in Sachet (1954). The suffixes A, B & C, added here, distinguish each specimen. No thin sections could be located in the Smithsonian collection from the three samples and a fresh polished thin section was prepared from each specimen. Each consists of a distinct basalt textural type, albeit with related petrographic affinities.

Electron microprobe analyses (EMPA) were made at the Geology Department, University of Auckland using a JEOL JXA-5A instrument operating at an accelerating voltage of 15 kV and an adsorbed sample current of c. 650 pA, with a Link Systems LZ-5 EDS detector. Raw data were corrected using a QX 2000 processor and ZAF-4/FLS quantification software version QX 20-24F-1291.

Chemical compositions of the three rocks were analysed by standard x-ray fluorescence (XRF) of Norrish fusion discs (majors) and pressed boric acid pellets (minors) after Parker (1994). The laser ablation analyses were performed using a 193 nm wave length ultraviolet Excimer laser facility in the Research School of Earth Sciences, Australian National University, Canberra, ACT, as outlined in Hoskin (1998).

Petrography

102227A. Holocrystalline olivine basalt. Partially resorbed olivine phenocrysts (<5%) and microphenocrysts of clinopyroxene and plagioclase (15%), and sparse ferromagnesian intergrowths are set in a pilotaxitic to intergranular, microporphyritic groundmass of feldspar laths (>40%), pyroxene (>20%), and ilmenite (s.l.) and magnetite (s.l.) granules (15%). Apatite needles, potash feldspar laths and quartz are scarce.

In composition olivine ranges $Fo_{76–72}$; feldspar groundmass laths and microphenocrysts $An_{60–55}$, inclusions $An_{65–55}$; clinopyroxene $Ca_{46–41}Mg_{47–41}Fe_{15–11}$. Fe-Ti oxides occur as flakes, cubes, octahedra, irregular grains and in intimate intergrowths in skeletal intergrowths. Pyroxene grains are generally angular, anhedral, and rarely rounded, colourless and rarely pleochroic (weak yellow). Elongated, twinned laths and irregular feldspar microlites have abundant inclusions. Some ferromagnesian minerals show oxidized rims.

Rounded, coarse-crystallized (doleritic or micrograbbroic) clots, up to 10 mm diameter, from 15–20% of the rock and are commonly enclosed by a discontinuous rim of euhedral-subhedral ulvöspinel (s.l.). Intergrown bladed plagioclase $An_{61–55}$ (40–55%), subhedral olivine ≈Fo_{75} (<5%), anhedral orthopyroxene $Ca_{2–5}Mg_{74–71}Fe_{23–28}$, clinopyroxene $Ca_{37–42}Mg_{43–47}Fe_{15–16}$, (15–20%), and coarse, acicular aggregations of Fe-Ti oxides (<10%), are ophitically enclosed by a mesostasis of brownish glass (10–30%) riddled with fine radiating needles, possibly rutile. In some smaller masses the silicate crystals radiate towards the centre. In others, small elongate feldspars at margins surround a coarser interior. Several of the clots appear linked through an incipient coarsening of the enclosing basalt. All resemble coarse segregations within the basalt, rather than cognate xenoliths of earlier crystallized rock. Similar "glomeroporphyritic clots of olivine and feldspar with subophitic pyroxene" appear in the Salani Volcanics of Upolu (Brothers, 1959, p. 40).

102227B. Coarse, altered, vesicular picrite basalt with a weathered outer rim, 5–10 mm thick, in which bioclastic carbonate infills vesicles.

Abundant olivine (>35%) phenocrysts and microphenocrysts, up to 5 mm diameter, are commonly subhedral. Most are partially resorbed and marginally altered, particularly the larger grains, with orange-stained iddingsitic rims and fractures. Many crystals show zoning and/or lamellae. Some (<5%) form in glomerocrysts with pyroxene and, rarely, plagioclase. Olivine compositions range $Fo_{88–75}$, but mostly $Fo_{78–75}$, without noticeable differences between phenocrysts, megacrysts, or in lamellated crystals. Zoned crystals show slight variations (e.g., core Fo_{83}, rim $Fo_{76)}$, but some large phenocrysts show cores up to Fo_{88}. Rare crystals show $Fo_{44–41}$.

Clinopyroxene forms glomerocrysts (e.g., $Ca_{45}Mg_{45}Fe_{10}$), phenocrysts (e.g., $Ca_{44}Mg_{45}Fe_{11}$) and intersertal grains (15–20%), where it accompanies stubby, irregular laths of plagioclase (35–45%), Fe-Ti oxides (5–10%), and murky (chloritized) glass (5–10%). The oxide phase(s) are too intergrown with both primary and secondary silicates for satisfactory electron microprobe analysis.

Plagioclase laths and rare feldspar microphenocrysts (zoned $An_{53–66}$) form an unoriented mat but are locally moulded about large olivines and glomerocrysts.

102227C. Fine-grained, vesicular, olivine-poor (<4%) basalt with 5% pyroxene, and <5% plagioclase phenocrysts and microphenocrysts and aggregations in a pilotaxitic to hylaopilitic groundmass. The latter forms a felt of ill-defined plagioclase laths (15%), microcrystalline Fe-Ti oxides (20%), fine granular pyroxene (10%), and dark glass and irresolvable material (40%). Numerous, small (<1 mm), feldspar-poor glomerocrysts of coarse ferromagnesian phases (8–12%) are seamed by the host basalt, but show irregular, angular and unresorbed margins.

Olivine ($Fo_{78–76}$) shows minimal zoning. It forms large (up to 2 mm) scattered, slightly resorbed euhedral crystals, smaller (0.05–0.2 mm) euhedral to anhedral phenocrysts and microphenocrysts, and rare glomerocrysts.

Clinopyroxene ranges from tabular, <1 mm diameter, euhedral phenocrysts ($Ca_{45–41}Mg_{46–39}Fe_{17–11}$), through microphenocrysts (e.g., $Ca_{46}Mg_{41}Fe_{13}$), to an intergranular microcrystalline groundmass phase (e.g., $Ca_{46}Mg_{43}Fe_{11}$) and is common in glomerocrysts (e.g., $Ca_{45}Mg_{44}Fe_{11}$). It is most iron-rich in some phenocryst rims.

Plagioclase is common as groundmass laths. Rare, large phenocrysts include one with an internal irregular reaction rim of opaque oxide. The laths show weak alignment, range in composition $An_{60–70}$ and rarely to An_{35}. Minor feldspar in glomerocrysts (<20%) ranges $An_{65–70}$.

Vesicle coatings include silicates as straw-coloured, flat subhedral and tabular euhedral clinopyroxene, possibly orthopyroxene, euhedral plagioclase and stumpy, subhedral anorthoclase (?). Other phases are dark bladed subhedral Fe-Ti oxides, white rosettes of a subhedral silica, possibly tridymite, and undetermined colourless, abundant, radiating, trigonal needles.

Table 1. Representative analyses and structural formulae of olivines from Rose Atoll basalts.

	1Ac	2Bc	2Br	3Bc	4Bc	5Br	6Br	7Br	8Bc	10B	11B	14Cc	15Cr
SiO_2	39.17	39.42	38.73	39.95	38.71	38.77	39.71	34.24	39.23	38.51	38.80	38.86	39.16
FeO	21.40	18.21	20.96	13.20	21.11	20.53	16.59	46.31	18.40	21.47	19.52	20.84	20.15
MnO	0.35	0.24	0.28	—	0.37	0.21	0.23	0.74	0.21	0.35	—	0.23	0.24
MgO	39.16	42.09	39.77	45.59	38.88	39.50	42.65	18.44	42.02	39.51	40.49	39.07	39.81
CaO	0.12	0.37	0.43	0.34	0.38	0.38	0.36	0.54	0.39	0.46	0.42	0.28	0.35
Total	100.20	100.33	100.17	99.08	99.45	99.39	99.54	100.27	100.25	100.30	99.23	99.28	99.71
Structural formulae on basis of 4(O)													
Si	0.994	1.001	1.000	1.003	1.010	1.005	1.012	1.011	0.996	0.996	1.002	1.010	1.010
Fe	0.454	0.387	0.453	0.277	0.461	0.445	0.354	1.143	0.196	0.465	0.422	0.463	0.435
Mn	0.008	0.007	0.007	—	0.009	0.005	0.013	0.019	0.005	0.008	—	0.005	0.006
Mg	1.481	1.795	1.530	1.705	1.512	1.513	1.620	0.812	1.590	1.523	1.559	1.514	1.531
Ca	0.003	0.010	0.012	0.009	0.011	0.011	0.010	0.017	0.001	0.013	0.012	0.008	0.010
X	2.01	2.00	2.00	1.99	1.99	1.99	2.00	1.99	2.00	2.01	1.99	1.98	1.98
Fo	76.5	80.5	77.2	86.0	75.9	77.4	81.2	40.8	80.3	76.6	78.7	76.5	77.3
Fa	23.5	19.5	22.8	14.0	24.1	22.6	18.8	59.2	19.7	23.4	21.3	23.5	22.7

A, B, C = specimens 102227A, 102227B, 102227C

c, core; *r*, rim; FeO = total iron as FeO (or Fe^{II}); *Fo*, forsterite; *Fa*, fayalite

Table 2. Representative analyses and structural formulae of pyroxenes from Rose Atoll basalts.

	Phenocrysts		Microphenocrysts			Groundmass	Glomerocrysts	Intergrowth	Dolerite clots				
	1Bct	**2Cc**	**4Cr**	**5A**	**7C**	**9B**	**11C**	**13A**	**14A-B1**	**16A-B1**	**18A-B2**	**19A-B2**	**20A-B3**
SiO_2	50.64	50.20	49.75	50.67	46.40	50.51	49.41	54.51	50.87	54.09	51.39	53.10	53.26
TiO_2	1.08	1.34	1.72	1.51	3.00	1.35	1.86	—	1.31	0.62	1.18	0.52	0.73
Al_2O_3	2.87	3.88	4.29	2.87	6.37	3.53	4.21	0.72	2.73	1.52	2.00	1.75	1.70
Cr_2O_3	0.62	—	—	—	—	—	—	—	—	—	—	—	—
FeO	6.49	5.79	6.60	8.92	7.65	6.65	6.33	17.30	10.03	14.60	8.56	14.95	14.69
MnO	—	0.24	—	0.34	—	0.23	—	0.77	0.40	0.47	0.24	0.63	0.43
MgO	15.50	15.66	15.22	15.77	13.53	14.72	15.18	25.73	14.62	27.04	16.14	26.65	27.06
CaO	20.92	21.62	21.25	20.27	21.41	21.58	21.57	1.41	19.89	2.19	19.73	1.96	1.90
Total	98.12	98.73	98.83	100.35	98.36	98.57	98.56	100.44	99.85	100.53	99.24	99.56	99.77
Structural formulae on basis of 6(O)													
Si	1.898	1.872	1.853	1.883	1.754	1.897	1.854	1.982	1.900	1.946	1.920	1.934	1.933
Ti	0.031	0.038	0.049	0.042	0.085	0.038	0.052	—	0.037	0.017	0.033	0.014	0.020
Al^{iv}	0.071	0.090	0.098	0.075	0.161	0.065	0.094	0.018	0.063	0.037	0.047	0.052	0.047
Al^{vi}	0.058	0.080	0.090	0.051	0.123	0.091	0.093	0.013	0.057	0.027	0.041	0.023	0.026
Cr	0.019	—	—	—	—	—	—	—	—	—	—	—	—
Fe	0.203	0.181	0.206	0.277	0.242	0.209	0.199	0.526	0.313	0.440	0.268	0.455	0.446
Mn	—	0.008	—	0.011	—	0.007	—	0.024	0.013	0.014	0.008	0.019	0.013
Mg	0.866	0.871	0.845	0.874	0.763	0.824	0.848	1.394	0.814	1.451	0.899	1.448	1.463
Ca	0.841	0.864	0.852	0.807	0.868	0.868	0.867	0.055	0.796	0.085	0.790	0.007	0.074
X+Y	1.985	2.004	1.993	2.020	1.996	1.999	2.007	2.012	1.993	2.017	2.006	2.022	2.022
Wo	44.0	44.9	44.8	41.0	46.4	45.7	45.3	2.8	41.1	4.3	40.4	3.8	3.7
En	45.3	45.3	44.4	44.4	40.7	43.3	44.3	69.7	42.1	72.9	45.9	71.7	73.8
Fs	10.7	9.8	10.8	14.6	12.9	11.0	10.4	27.5	16.8	22.8	13.7	24.5	22.5

A, B, C, = 102227A, 102227B, 102227C; *t*, twinned grain; *c*, core; *r*, rim; *B1, B2, B3,* different doleritic clots; *Wo*, wollastonite; *En*, enstatite; *Fs*, ferrosilite.

Mineralogical observations

Representative EMP analyses of the major phases in the three samples are given in Tables 1–4.

Olivines (Table 1). The representative olivine analyses are typical of alkali basalts in Samoan rocks (Macdonald, 1944; Stice, 1968; Natland & Turner, 1985). Compositions mostly lie between Fo_{82} and Fo_{72} with samples A and C showing restricted resorption and compositional zoning in their crystals (analyses 1,14–15).

In contrast, the picrite, 102227B, shows wider olivine compositions (analyses 2–8, 10–11). Most range within $Fo_{88–75,}$ zoning is common (analyses 2,3,5,6). This is typical in Samoan basalts, along with Fe-rich crystals ($Fo_{44–41}$) e.g., analyses 7 (cf. Macdonald, 1944; Natland & Turner, 1985). Thus olivine in 102227B indicates a complex crystallization; both the lamellar olivines and the iron-rich varieties may represent xenocrysts.

Pyroxenes (Table 2). The clinopyroxene compositions cluster in the quadrilateral $Ca_{47}Mg_{43}Fe_{10}$-$Ca_{47}Mg_{36}Fe_{17}$-$Ca_{40}Mg_{43}Fe_{17}$-$Ca_{40}Mg_{50}Fe_{10,}$ as is typical in the alkalic and tholeiite basalts of the Fagaloa shield volcano of Upolu (Natland & Turner, 1985). However, more Ca-rich pyroxenes from Fagaloan lavas contain less Fe than some Rose analyses.

Groundmass pyroxenes in 102227B (analysis 9) are Ca-rich ($\geq Ca_{45}$) and range from Fe_{10} to Fe_{14}, as are some microphenocrysts from A and C, cores of phenocrysts, and glomerocrysts, from samples B and C (analyses 1–2, 11). Phenocryst cores of augite ($\approx Ca_{41}$) in C and microphenocrysts in A are less common, but also display Fe-values similar to the main compositional range (analysis 5). Only rims of some phenocrysts in A are more extreme (analysis 4Cr). Although titanaugites are known in Samoan lavas (e.g., Macdonald, 1944; Brothers, 1959; Stice, 1968; Natland & Turner, 1985), in only one spot Rose analysis (analysis 7) did TiO_2 exceed 1.9 wt%. The negligible Na in the Rose clinopyroxenes is an unusual feature, but is recorded in rare tholeiitic lavas in Upolu basalts (Natland & Turner, 1985). Chromium was detected in only two clinopyroxene crystals from Rose samples.

A rare intergrowth of orthopyroxene in clinopyroxene in A gave $Ca_3Mg_{70}Fe_{27}$ (analysis 13). No pigeonite was found (cf. Natland & Turner, 1985). The clinopyroxenes of the coarser clots in B all plot at or beyond the Ca_{40} margin of the main field (analyses 14A,18A). In composition ($Ca_{40–41}$ $Mg_{42–46}$ $Fe_{14–17}$), they coexist with orthopyroxenes ($Mg_{71–74}$ $Fe_{22–26}$ $Ca_{3–4}$) with significant Ca (analyses 16, 19–20). Calculated Wood & Banno (1973) temperatures for these coexisting pyroxene compositions range 1021–1088°C; Wells (1977) temperatures are 1030–1126°C.

Feldspars (Table 3). Plagioclase in the three rocks ranges from $An_{70}Ab_{29}Or_1$ to $An_{53}Ab_{43}Or_3$. Those in A lie at the Na- and K-rich end (analysis 1), those in B span the entire range and those in C are skewed towards the middle and Ca-rich end (analyses 5–7, 16–17). Microphenocrysts in A (analyses 8,9) and the feldspars in its clots (analyses 10–12) overlap the groundmass feldspar compositions. However, the microphenocrysts are the most Ca-rich feldspars, while feldspars in the clots tend towards the Na- and K-rich end of the range. Most feldspars are inhomogeneous and Fe and a little Ti may partly reflect minute Fe-Ti oxide inclusions.

K-rich oligoclase is common as an interstitial phase in some Samoan lavas (Macdonald, 1944; Brothers, 1959), but only one such composition was found herein ($Ab_{36}An_{51}Or_{12}$).

Table 3. Representative analyses and structural formulae of feldspars from Rose Atoll basalts.

	Groundmass laths					Microphenocrysts		Ex dolerite inclusions			Ex glomerocrysts		
	1A	**2B**	**5C**	**6C**	**7C**	**8A**	**9A**	**10A**	**11A**	**12A**	**16C**	**17C**	**18B**
SiO_2	54.24	54.09	51.70	52.51	50.34	54.67	52.22	54.74	53.36	54.84	51.03	50.69	60.46
TiO_2	0.19	0.25	0.19	0.23	—	0.22	—	0.18	—	0.18	—	—	0.26
Al_2O_3	27.36	27.72	29.29	28.83	30.50	27.47	29.44	28.23	28.35	27.48	29.67	30.44	23.07
FeO	0.87	0.91	1.00	1.05	0.81	0.85	0.97	0.87	1.14	0.80	0.61	0.64	0.61
CaO	10.96	10.76	12.82	12.23	14.08	10.65	13.02	11.37	12.11	10.88	13.64	14.21	5.16
Na_2O	4.64	4.79	3.71	4.32	3.28	4.44	3.73	4.51	3.96	4.61	3.70	3.08	5.85
K_2O	0.69	0.57	0.24	0.38	0.17	0.74	0.47	0.63	0.51	0.77	0.18	0.16	3.49
Total	98.95	99. 09	98.95	99.55	99.18	98.98	99.85	100.53	99.43	99.56	98.83	99.22	98.90
Structural formulae on basis of 32(O)													
Si	9.952	9.898	9.520	9.613	9.267	9.997	9.530	9.875	9.760	9.987	9.437	9.315	
Ti	0.026	0.035	0.026	0.032	0.013	0.032	0.019	0.026	0.013	0.026	0.003	0.019	
Al	5.917	5.981	6.358	6.221	6.618	5.907	6.333	6.003	6.112	6.898	6.404	6.592	
Fe	0.134	0.138	0.154	0.160	0.125	0.128	0.147	0.131	0.173	0.122	0.093	0.992	
Ca	2.157	2.109	2.531	2.397	2.778	2.086	2.547	2.198	2.374	2.125	2.701	2.800	
Na	1.651	1.699	1.325	1.533	1.171	1.574	1.318	1.578	1.402	1.626	1.325	1.098	
K	0.160	0.134	0.054	0.090	0.042	0.173	0.109	0.147	0.118	0.179	0.045	0.035	
Z	16.03	15.91	16.05	16.03	16.03	16.06	16.03	16.03	16.06	16.03	15.94	16.02	
X	3.97	3.94	3.91	4.02	3.99	3.83	3.97	3.93	3.89	3.93	4.07	3.93	
An	54.4	53.5	64.8	59.6	69.6	54.4	64.1	56.0	61.0	54.1	66.4	71.2	
Ab	41.6	43.1	33.8	38.2	29.3	41.1	33.2	40.2	36.0	41.4	32.5	27.9	
Or	4.0	3.3	1.4	2.2	1.1	4.5	2.7	3.8	3.0	4.5	1.1	0.9	

A, B, C = 102227A, 102227B, 102227C. *An*, anorthite; *Ab*, albite; *Or*, orthoclase normative components.

Fe-Ti oxides (Table 4). Two groups of Fe-Ti oxides occur in the samples: a Ti-poor Fe-rich spinel phase, presumably magnetite, and a Ti-rich ulvöspinel phase with Fe^{2+}»Fe^{3+} (based on stoichiometry). Only the Fe-Ti oxides in A gave consistent electron microprobe results. Representative examples in Table 4 have the structural formulae recalculated after Droop (1987) to partition total iron between Fe^{2+} and Fe^{3+}. An alternative method by Carmichael (1967) gives a magnetite-rich phase with 20.9 to 16.7 mol % ulvöspinel and a Ti-rich oxide phase with from 15.6 % R_2O_3 in 2du, through 2.1% R_2O_3 in 1bl, to zero in 5d.

Natland & Turner (1985) report two opaque oxide solid solutions in the tholeiitic and alkalic basalts of Fagaloa, Upolu: an ilmenite-hematite solid solution and a magnetite-ulvöspinel solid solution. However, these differ from those in 102227A. In particular the alkalic Fagaloa lavas show a complete gradation in Fe^{3+} and Ti, between phenocrystalline magnesiochromite and groundmass magnetite-ulvöspinel solid solution; Cr_2O_3 (and V_2O_3) is negligible in the Rose sample. Further, among Fagaloa analyses, with comparable TiO_2 levels to the Ti-rich Rose oxides (only 4 out of 19 analyses), Al_2O_3 was markedly lower, although MgO and MnO were similar or less. In contrast, a single Fagaloa analysis with a similar TiO_2 level to the Ti-poor Rose oxides, showed a far greater Al_2O_3, a lower MgO, but ≈15 wt% Cr_2O_3. The remaining 14 Fagaloa analyses all had TiO_2 values well above those in 102227A. Nevertheless 102227A, like many of the Fagaloa lavas (Natland & Turner, 1985) has crystallized abundant Ti-bearing oxides, albeit of different composition, rather than incorporating Ti in the clinopyroxene.

Coexisting magnetite-ulvöspinel and hematite-ilmenite in a multiphase crystal in 102227A were analysed (2du, 2br). The results give ≈720°C and fO_2 ≈10^{-15} atm when plotted on the experimentally determined curves of Buddington & Lindsley (1964, fig. 5). In the coarser clots both Ti-poor and Ti-rich oxide phases are present but textural relations indicate separate crystallization; the spinels occur at the clot rims as reaction products, while the ulvöspinel-rich phases lie within the clots, where siliceous liquid could have afforded an oxygen buffer (cf. Carmichael, 1967).

Table 4. Representative analyses and structural formulae (after Droop, 1987), Fe-Ti oxides from Rose Atoll basalt 102227A.

	1bl	**2du**	**5d**	**6d**	**2br**	**8d†**
SiO_2	0.47	0.42	0.41	0.44	0.56	0.45
TiO_2	52.30	46.33	51.49	31.88	6.72	5.75
Al_2O_3	1.56	0.22	1.33	0.50	3.87	2.87
Fe_2O_3	*	15.64	*	33.03	42.10	43.59
FeO	37.59	28.89	37.79	29.65	40.41	43.64
MnO	0.25	0.51	—	—	0.42	0.50
MgO	3.34	7.67	3.27	2.50	3.73	2.62
CaO	—	—	0.13	0.13	—	—
Total	95.51	99.68	94.42	98.13	97.81	99.42
Structural formulae on basis of 24 cations						
Si	0.144	0.108	0.132	0.132	0.163	0.132
Ti	12.036	10.032	12.036	7.329	1.488	1.268
Al	0.564	0.072	0.480	0.179	1.343	0.992
Fe^3	*	3.396	*	7.599	9.322	9.626
Fe^2	9.624	6.972	9.828	7.582	9.943	10.709
Mn	0.060	0.120	—	—	0.105	0.126
Mg	1.560	3.300	1.512	1.136	1.635	1.146
Ca	—	—	—	0.042	—	—

bl, bladed grain; *du*, least reflectant area of composite skeletal gain; *br*, most reflectant area of skeletal composite grain; *d*, grains from doleritic clots; † grains from clot rims; * total iron as FeO (or Fe^2).

Chemistry

The XRF analyses, and CIPW norms, for the three samples are given in Table 5. Semiquantitative analysis for chlorine showed some 2200 ppm in 102227B point to slight seawater contamination. This rock also contains small amounts of encrusting bioclastic carbonate debris in its vesicles.

The three samples represent contrasting basalt types: 102227A is gradational to quartz tholeiite, with 21% normative Hy and 1% Q, slightly evolved *mg* value (60), and a *DI* of 21; 102227B plots as a picrobasalt (Le Maitre, 1984) with high normative Ol (23%), minor Hy (<1%), an *mg* value typical of primitive or cumulate basalts (70), and a *DI* of 18; 102227C is transitional olivine basalt with normative Ol (6%) and Hy (7%), a moderately evolved *mg* value (57), and *DI* of 26. Electron microprobe analysis of tholeiite A glass (Agl Table 6) shows it to be potash- and silica-rich, and rhyolitic in normative composition with 27–39% Q. The glass shows low totals suggesting 4–6% volatiles (Table 6) and strong Rb, Th, U, K, La, Zr enrichment and Ba, Ti, Sr depletion relative to the host basalt (Table 7).

The three samples resemble other Samoan basalts and to date are closest to Ta'u island lavas (Stice, 1968; Hubbard, 1971) from the nearest volcano in the adjacent Manu'a Group (Table 8, Figs. 2, 3). Importantly, both Rose and Ta'u basalts differ from western Manu'a Group basalts of the Ofu and Olosega islands, which are more enriched in Ti relative to Al (Hubbard, 1971). The Al_2O_3/TiO_2 ratios of the Rose samples are typical of most Samoan chain basalts (cf. Macdonald, 1968; Hawkins & Natland, 1975; Natland & Turner, 1985; Johnson, *et al*., 1986). Only examples from the Lalla Rookh Bank (Johnson *et al*., 1986) show the lower Al_2O_3/TiO_2 found in western Manu'a islands lavas.

Yet, despite geochemical similarities between Rose and Ta'u basalts (Table 8, Figs. 2, 3), some differences exist, particularly in Sr vs P_2O_5 and Ni vs MgO (Figs. 4, 5). Although this could reflect sampling bias, no rock corresponding to 102227A was reported from the Manu'a islands by Stice (1968) despite prominent tholeiites among Samoan shield basalts west of Manu'a (Natland & Turner, 1985). One picrite basalt no. 131 from Ta'u (Stice, 1968) has transitional tholeiitic affinities, but higher SiO_2 and Hy

Table 5. Analyses and CIPW norms Rose Atoll basalts and averaged glass (*Agl*) from within doleritic clots of sample A (Tables 6 and 7).

	A	B	C	Agl*
SiO_2	46.77	44.29	46.40	70.59
TiO_2	3.93	2.97	3.92	0.85
Al_2O_3	12.83	10.22	13.89	13.07
Fe_2O_3t	13.41	14.09	13.05	0.69
MnO	0.19	0.18	0.18	—
MgO	8.24	13.56	6.89	0.01
CaO	10.65	11.33	11.20	0.99
Na_2O	1.75	1.59	2.51	2.10
K_2O	0.86	0.70	0.81	6.48
P_2O_5	0.70	0.36	0.47	—
Total	99.33	99.30	99.32	95.08
t, total Fe as Fe_2O_3 * includes 0.30 Cl				
CIPW normative composition				
Q	1.01	—	—	34.45
C	—	—	—	1.23
Or	5.12	4.17	4.82	40.24
Ab	14.91	13.55	21.38	16.70
An	24.78	18.82	24.41	5.16
Mt	3.91	4.12	3.81	—
Hm	—	—	—	0.18
Il	7.51	5.68	7.50	—
Ru	—	—	—	0.18
Ap	1.67	0.86	1.12	—
Di	19.23	28.41	23.06	—
Hy	20.81	0.43	6.97	0.03
Ol	—	22.85	5.91	—
Hl	—	—	—	0.43
mg	60.3	70.4	56.6	2.8
DI	21.0	17.7	26.2	91.4

	A	B	C	Agl
Sc	29	30	33	<8
V	337	310	344	<3
Cr	357	884	200	<3
Ni	131	366	93	61
Cu	25	69	89	24
Zn	118	115	120	nd
Ga	23	17	24	nd
Rb	29	13	14	240
Sr	484	390	521	80
Y	42	25	37	41
Zr	365	195	274	638
Nb	57	29	36	60
Ba	273	165	211	509
La	57	24	35	79
Pb	6	4	3	nd
Ce	128	54	73	158
Th	6	1	5	23
U	3	7	2	6
Normative mineralogy				
Clinopyroxene				
Wo	51.7	42.1	51.5	—
En	33.2	35.6	31.9	—
Fs	15.1	12.4	16.6	—
Orthopyroxene				
En	68.6	74.2	65.7	100.0
Fs	31.4	25.8	34.3	—
Olivine				
Fo	—	73.2	3.5	—
Fa	—	27.7	65.0	—
Plagioclase				
Ab	37.6	29.6	3.3	76.4
An	62.4	70.4	6.7	23.6

Normative symbols after Hutchison (1974), with norms calculated from anhydrous analyses recalculated to 100% with $Fe_2O_3/(FeO+Fe_2O_3)$ set to 0.20. *mg*, $Mg/(Mg+Fe^{2+})\times100$. *DI*, Differentiation Index (Σ Q, Or, Ab).

Table 6. EMP analyses of glassy mesostasis, doleritic clots in 102227A.

	inclusion 1		inclusion 2		inclusion 3	
	1	2	3	4	5	6
SiO_2	70.27	71.89	69.98	71.06	70.37	70.01
TiO_2	0.77	0.70	1.04	0.92	0.78	0.91
Al_2O_3	12.87	13.08	13.27	12.20	13.54	13.47
FeO*t*	0.91	0.74	0.71	0.49	0.59	1.15
MgO	—	—	—	0.05	—	—
CaO	0.77	0.81	1.72	0.77	0.84	1.01
Na_2O	2.22	2.21	2.96	1.68	1.94	1.56
K_2O	6.03	6.23	4.54	6.46	7.06	8.53
Cl	0.34	0.28	0.23	0.30	0.35	—
P_2O_5	—	—	—	—	—	—
Total	94.18	95.94	94.45	93.93	95.47	96.64
t, total Fe as FeO.						
CIPW norms						
Q	36.48	36.66	34.80	38.68	33.57	27.13
Or	37.84	38.88	28.41	40.67	43.70	52.16
Ab	17.28	17.33	24.72	12.78	14.48	13.66
An	4.06	4.19	9.03	4.07	4.36	4.72
C	1.89	1.70	0.73	1.57	1.76	—
Wo	—	—	—	—	—	0.20
Mt	0.12	—	—	—	—	0.34
Hm	0.13	0.17	0.17	0.12	0.14	0.03
Il	1.55	1.30	1.27	0.88	1.04	1.79
Ru	—	0.04	0.43	0.52	0.27	—
Hl	0.60	0.48	0.40	0.53	0.60	—
Hy	—	—	—	0.13	—	—

Norms calculated from anhydrous analyses recalculated to 100% with $Fe_2O_3/(FeO+Fe_2O_3)$ set to 0.20.

than the Rose picrite basalt B. Intriguingly, the alkalis and silica of 102227A are in similar proportions to the recalculated composition of Stice's picrite basalt no. 131, if all normative Ol is subtracted from the original composition. Further, both the total alkalis and titania of A are lower than in comparable picrites from Manu'a. Only 102227C bears some chemical comparison with Manu'a lavas (e.g., Stice, 1968; no. 117), but direct resemblances between Manu'a and Rose basalts are not clear.

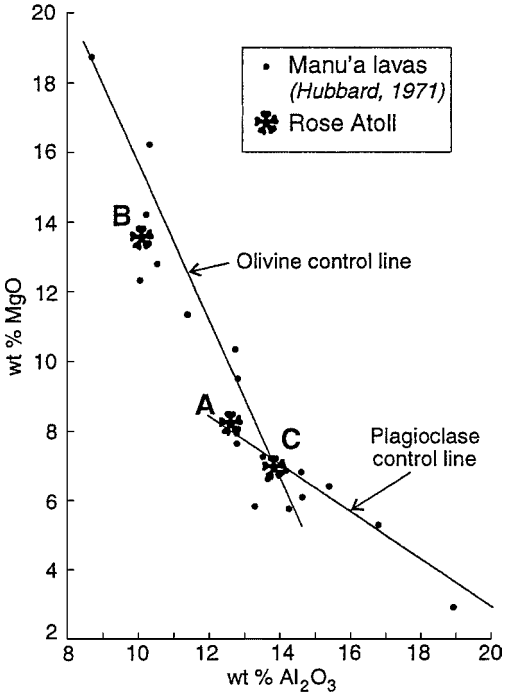

Fig. 2. Al_2O_3 vs MgO for Manu'a lavas and Rose Atoll samples. The olivine and plagioclase control lines are those of Hubbard (1971).

Incompatible elements in Rose basalts are compared in a mantle normalized diagram (Fig. 6). The elements are normalized to primitive mantle (PM) values and compared with enriched mid ocean ridge basalt (E-MORB) and low $^{87}Sr/^{86}Sr$ ocean island basalt (OIB), after Sun & McDonough (1989). The Rose basalts are relatively depleted in K and Sr and relatively enriched in U, Pb and La; they show variable enrichment in Rb, Ba, Th and P. The Ba/Nb and La/Nb ratios are compared in Fig. 7, which relates OIB fields to their $^{87}Sr/^{86}Sr$ isotope levels with increasing sedimentary crustal components in their source (Sun *et al*., 1989). Rose basalts plot from near the N-MORB field towards E-MORB (Ba/Nb 6.86 La/Nb 0.76) and low $^{87}Sr/^{86}Sr$ OIB (Ba/Nb 7.29, La/Nb 0.77) values, but do not intersect any major plume related OIB field.

Table 7. Laser ablation ICP-MS analyses of glass in doleritic clots in basalt 102227A.

	spot-1	spot-2	spot-3		spot-1	spot-2	spot-3
Li	< 6	< 2	< 8	La	80(10)	28(4)	128(18)
Sc	< 10	< 3	< 12	Ce	164(21)	55(7)	255(31)
V	< 4	< 1	< 5	Pr	19(3)	6.4(0.9)	28(4)
Cr	< 4	< 1	< 5	Nd	72(12)	24(4)	103(16)
Ni	62(16)	26(6)	95(42)	Sm	12(4)	5(1)	18(5)
Rb	234(23)	75(10)	411(50)	Eu	1.9(0.7)	1.0(0.3)	2(1)
Sr	50(7)	100(11)	90(14)	Gd	10(3)	4(1)	14(4)
Y	44(5)	14(3)	65(9)	Tb	1.4(0.4)	0.5(0.2)	2.2(0.8)
Zr	625(67)	227(28)	1061(123)	Dy	9(2)	2.7(0.8)	13(3)
Nb	56(10)	22(4)	101(15)	Ho	1.4(0.5)	0.6(0.2)	2.5(0.9)
Ba	458(50)	200(25)	869(96)	Er	5(1)	1.6(0.5)	6(2)
Ta	4.2(0.8)	1.4(0.3)	6(1)	Tm	0.7(0.3)	0.2(0.1)	0.8(0.4)
Th	22(2)	8(1)	38(5)	Yb	4(2)	1.6(0.5)	6(2)
U	5.6(0.9)	1.9(0.4)	10(1)	Lu	0.5(0.2)	0.2(0.09)	0.9(0.4)

Precision for ICP-MS laser ablation analyses given in brackets.

Table 8. Comparative Rose Atoll and Manu'a Islands (Ta'u) basalt compositions.

	Rose av.	Manu'a[a] av.	Manu'a[b]
SiO_2	45.8	45.5	45.8
TiO_2	2.6	3.5	3.4
Al_2O_3	12.3	12.3	12.7
FeO*t*	13.5	12.5	12.0
MnO	0.2	—	0.2
MgO	9.6	10.5	9.5
CaO	11.1	10.8	11.5
Na_2O	1.9	2.5	2.3
K_2O	0.8	0.8	0.9
P_2O_5	0.5	0.5	0.4
Ni	197	373	315
Sr	465	468	400
Zr	278	230	232
Rb	19	17	16

t, total Fe as FeO.

Ranges

La	24–57	27–40?
Sr	390–521	330–510
Ce	54–128	54–76
Ni	93–366	88–755
Zr	195–365	175–440
Rb	13–29	9–27
K/Rb	245–479	350–?

[a] excluding hawaiites; [b] basalt with similar MgO to Rose av. (Ab > An).

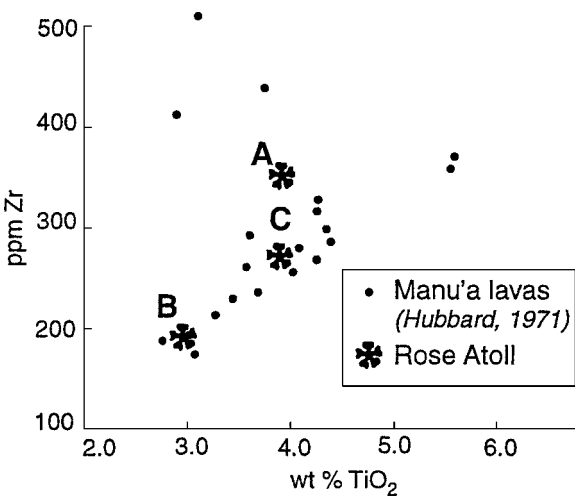

Fig. 3. TiO_2 vs Zr for Manu'a lavas and Rose Atoll samples.

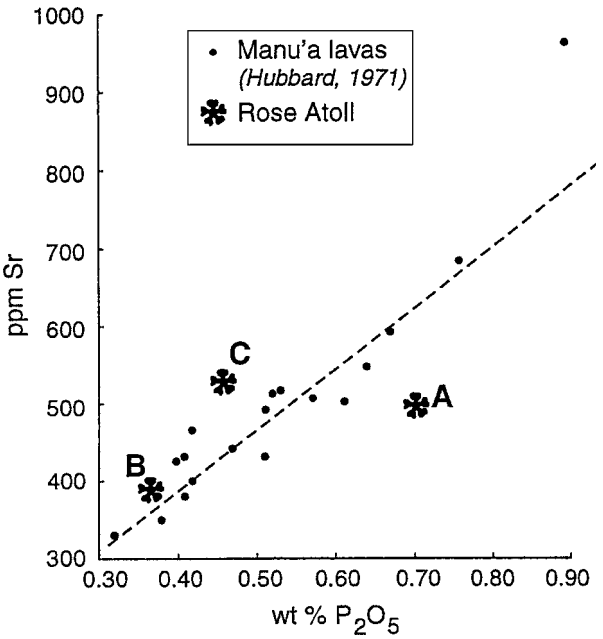

Fig. 4. Sr vs P_2O_5 for Manu'a lavas and Rose Atoll samples. Trend line from Hubbard (1971).

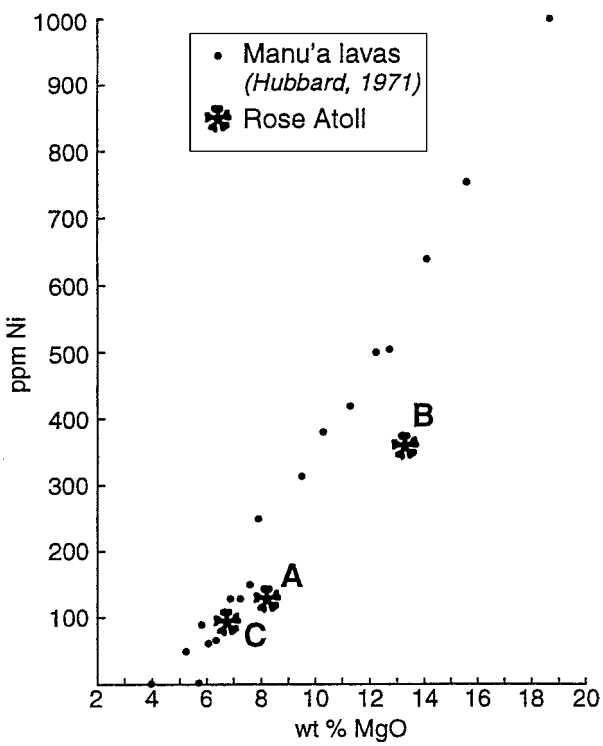

Fig. 5. Ni vs MgO for Manu'a lavas and Rose Atoll samples.

Table 9. Comparative trace element ratios for Rose Atoll basalts, N- and E-type MORB, low $^{87}Sr/^{86}Sr$ OIB, EM-OIB and HIMU basalts.

	Nb/Pb	Ce/Pb	Nb/U	K/U	K/Nb	Nb/Th
Rose Atoll A	9.5	21.3	19.0	2367	125	9.5
Rose Atoll B	7.3	13.5	3.4	829	200	29.0
Rose Atoll C	12.0	12.0	18.0	3350	186	7.2
N-MORB	7.5	25	50	12766	258	19.4
E-MORB	13.8	25	46	11677	253	13.8
Low $^{87}Sr/^{86}Sr$ OIB	15	25	47	11765	250	12.0
EM-OIB (Range)	8.3–15.9	14.5–31	40–43	5660–13700	270–430	6.3–11.5
HIMU (Range)	18–23	29–33	43–88	6000–8000	160–180	10–17

Data compiled from this paper and Sun & McDonough (1989).

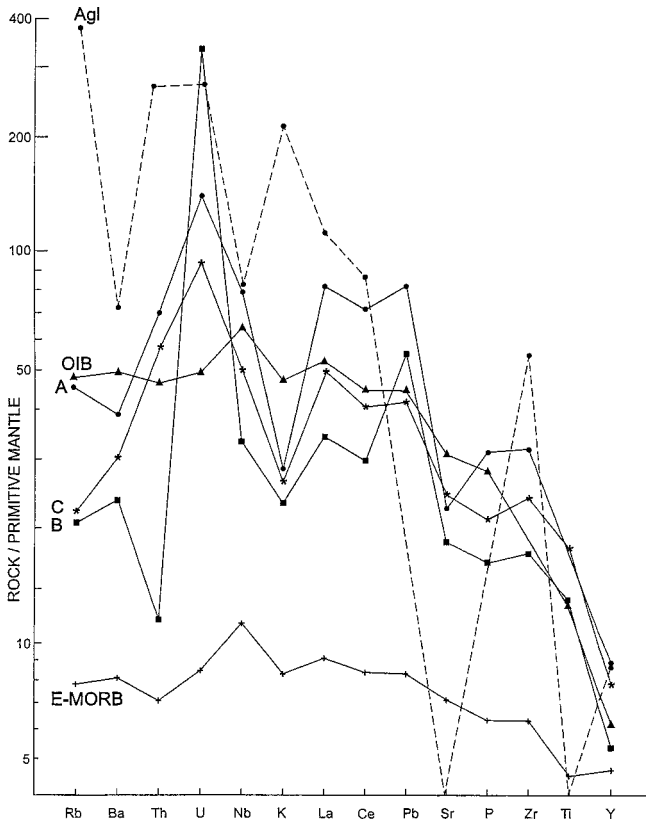

Fig. 6. Incompatible trace element plots of Rose Island basalts (A, B, C) normalized to primitive mantle, using normalization factors and data after Sun & McDonough (1989). Plots for enriched-type MORB and low $^{87}Sr/^{86}Sr$ OIB are shown for comparison.

Petrogenesis

Average Rose Island basalt shows lower MgO (1%), TiO_2 (0.9%) and Na_2O (0.6%) and higher FeO* (1%) than average Manu'a's Island's (Ta'u) basalt and TiO_2, FeO and Na_2O remain higher at equivalent MgO contents (Table 8). A more magnesian Manu'a's Islands parent would explain the higher Ta'u Ni contents. Petrologically, however, both Rose and Ta'u transitional to tholeiitic basalts suggest greater degrees of partial mantle melting than for basanites and nephelinites that characterize the young post-erosional Samoan volcanoes and seamounts (Hawkins & Natland 1975). The question then arises as to whether these young easternmost volcanoes reflect the asthenospheric/lower mantle plume activity of the older Samoan shields and Vailulu'u undersea volcano (Hart *et al.*, 2000).

Samoan plume magmatism is considered responsible for:

- the observed linear age progression in the shield volcanism for several Samoan islands (Natland & Turner, 1985; McDougall, 1985; Hart *et al.*, 2000);
- the isotopic character of shield basalts, where Sr, Nd and Pb isotopes are consistent with isotopic values of other Pacific island chains assigned to plume sources (Hedge *et al.*, 1972; Wright & White, 1987);
- a primitive helium isotopic mantle component in shield basalts (Farley *et al.*, 1992);
- mantle carbonatitic metasomatism identified in peridotite xenoliths contained in post-shield lavas (Hauri *et al.*, 1993).

The Rose basalts partly overlap the alkali basalt compositional range of the present plume-related Vailulu'u seamount (Hart *et al.*, 2000) in SiO_2 and MgO, but are distinctly lower in alkalis (Na_2O+K_2O 2.6–3.3 cf 3.5–5.9 wt %). This may reflect greater degrees of partial melting for Rose basalts. Rose basalts overlap and show a similar fractionation trend to other Samoan island basalts for Nb vs Zr (Fig. 8), except for the late-stage groundmass fractionation to silicic glass in the tholeiitic basalt (102227A) and both groups differ from the Combe Bank trend, which show elevated Nb/Zr. In Ba vs. Zr plots, Rose basalts differ in their fractionation trend to Samoan islands, Lalla Rookh Bank, Wallis Island, Combe Bank and Alexa Bank fields (Fig. 8).

No overlap in Ba/Nb vs. La/Nb exists between Rose basalts and the plume-related Samoan, Hawaiian or Atlantic fields (Fig. 7). In this respect Rose basalts differ from Wallis Island basalts, which fall within the Samoan plume field. Rose Ba/Nb and La/Nb values do not suggest high levels of crustal sedimentary components, while late-stage fractionation trends in tholeiite (102227A) to silicic glass (Agl) mostly increases La/Nb values.

A present Samoan plume position near Manu'a Group islands some 100km to 150km east of Tutuila was deduced on migration rates from shield volcano ages (Duncan, 1985; Natland & Turner, 1985; McDougall, 1985). Reconstructed plate motion tracks for two extreme plume positions relative to Manu'a and Rose islands (Fig. 9) are based on revised plate motion relative to Pacific "hotspots" (Gaina *et al.*, 2000; R.D. Müller, pers. comm., 2000). A Manu'a plume position more closely matches shield ages along the Samoan islands and the postulated plume at Vailulu'u submarine volcano, 45 km E of Ta'u Island. A Rose Atoll plume position gives ages 2 myr older than observed ages. Clearly, Rose Atoll lacks temporal or geochemical evidence for a Samoan plume input. Isotope data are not available for Rose basalts, but Sr isotopes for Ta'u ($^{87}Sr/^{86}Sr$ 0.7042–0.7050) are among the lowest recorded for Samoan basalts, while Ta'u and Vailulu'u record the highest $206Pb/^{204}Pb$ (192–194) values (Hart *et al.*, 2000). These values extend towards other Samoan shield values, but most shield and in particular "post-erosional" lavas show higher $^{87}Sr/^{86}Sr$ and lower $^{206}Pb/^{204}Pb$ values (Wright & White, 1987; Hart *et al.*, 2000).

Rose trace element ratios show little correspondence to end member MORB and OIB values (Table 9) perhaps reflecting an unusual or mixed lithospheric source. The Zr/Nb ratios for Rose basalts follow the Samoan shield crystal fractionation differentiation trend (Fig. 8), but initial Zr/Nb may stem from binary mixing of depleted MORB and other more enriched end members (Kamber & Collerson, 2000). Other element ratios for Rose basalts (Rb/Sr 0.027–0.060, U/Pb 0.50–1.75, Th/Pb 0.25–1.64) generally overlap typical Hawaiian tholeiitic data (Rb/Sr 0.278, U/Pb 0.56–2.11, Th/Pb 2.09); this precludes an abnormal, overwhelming Mid-Ocean Ridge imprint, as found in the Detroit seamount along the Hawaiian plume trace (Keller *et al.*, 2000).

Discussion

Of the different basalt types documented from the Samoan Island chain, the three Rose Atoll samples collected by Schultz conform most closely to the Ta'u Island basalts of the neighbouring Manu'a Group. However, differences exist and any similarities in petrography and chemistry are typical

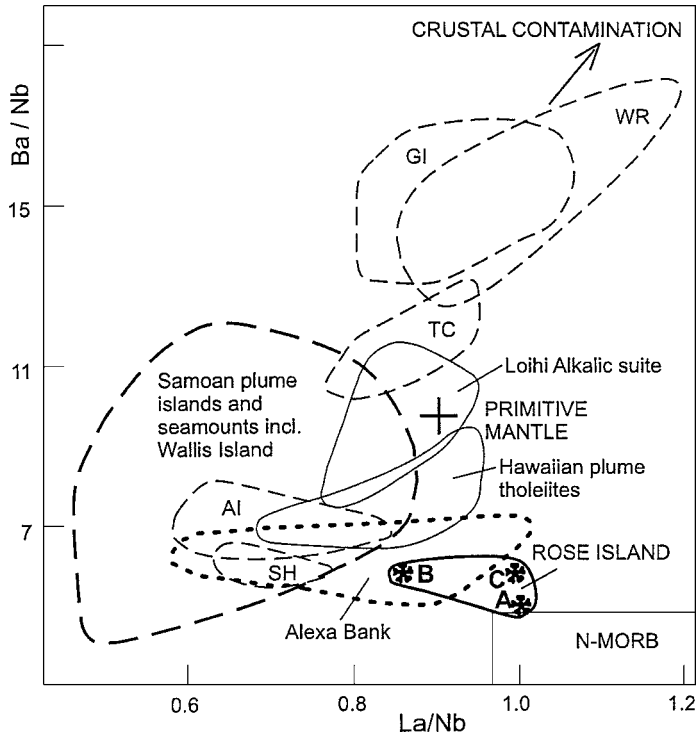

Fig. 7. Ba/Nb vs La/Nb diagram of Rose Atoll basalt plots related to N-MORB, Primitive Mantle (cross) and fields of Pacific and Atlantic plume basalts (based on Sun & McDonough, 1989). Solid thick line: Rose Atoll basalt field; thick dotted line: Alexa Bank field; solid thin line: Hawaiian plume tholeiites and Loihi alkalic to transitional basalt fields; thin dashed lines: Atlantic plume basalt fields (St Helena SH, Ascension Island AI, Tristan da Cunah TC, Gough island GI, and Walvis Ridge WR). Rose Atoll data (A, B, C and Agl) from this paper. Samoan plume islands and seamount fields (9 analyses) from Johnson *et al*. (1986) and Wallis Island (12 analyses) from Price *et al*. (1991). Hawaiian plume tholeiites (19 analyses, excluding Koolau and other separate source basalts) from Norman & Garcia (1999). Loihi alkalic to transitional basalts (20 analyses) from Garcia *et al*. (1995).

of those to be expected among geographically contiguous basalts formed within a single evolving petrographic province. Only one Rose sample shows distinct affinities with any of the rock types documented from the eastern Manu'a Group. As such, no unambiguous evidence presently exists that the three described rocks might have been transported to Rose; an inference consistent with the large size of some specimens recorded by Wilkes (1844) and Dana (1849). The chemistry of the rocks generally conforms with that expected from a young volcano in the Samoan chain but their precise characters pose a number of questions.

Both Rose and Ta'u basalts lie near the eastern plume limits for Samoan activity. Both resemble Wallis Island basalts in age (<1Ma) and petrological spectrum, except that Wallis lavas display the presence of a plume component that reflects their island's position within the previous Samoan plume path (Stice, 1968; Natland & Turner, 1985; Price *et al*., 1991). Wallis Island activity is attributed to a thermal disturbance in the lithosphere some 9 myr after plume passage, possibly from tectonism near a Pacific-Australian transform boundary. Rose Atoll is distant from this tectonic feature and hence its origin is enigmatic. Its activity may stem from late differential flexure and rifting and volcanic loading along the Samoan chain (Savi'i, Upolu, Tutuila) that involved production of "post-erosional" eruptives (Natland & Turner, 1985), although the height of the atoll and its petrological span may be too large for such an exclusive origin. Adjustments in the stress field beyond this zone however, may have focused melting in lithosphere beneath the Manu'a and Rose region, prior to resurgence of the Samoan plume at Vailulu'u seamount.

Origin of the Samoan chain has been controversial due to its limited migratory progression, complex eruptive pattern and its unusual mantle geochemical signatures (Natland, 1980; White & Hofmann, 1982). However recent studies support plume input (Hart *et al*., 2000). Removal of Rose (and Ta'u) volcanism from plume input suggests plume activity has become more sporadic since earlier more western Samoan plume volcanism. One possibility is for a fast plume, as modelled by Larsen & Yuen (1997). Such plumes last for less than 8 myr and are initiated when subducted slabs grade into horizontal flow in the lower mantle. However subduction and downthrusting along the Pacific-Australian plate margin is away from the Samoan chain in this region, which presents a difficulty for a fast plume origin. A recent study has proposed that linear Pacific volcanic chains may show progressive plume eruptive ages mixed with non-progressive activity (Hieronymous & Bercovici, 1999). In these cases the volcano spacing and irregular infillings are controlled by tectonic and flexural stresses on magma transport. Whether such a model applies to the Samoan Islands needs more detailed age dating and dynamic modelling studies of the volcanic evolution.

The basalt float sampled from Rose Atoll shows petrological attributes that link the rocks generally with neighbouring Ta'u Island. Some petrological distinctions, however, are known and this with size and distribution of such rocks on Rose does not favour their transport to Rose. Even if transport to Rose Atoll were to be demonstrated, knowledge of the particular characters of these rocks, along with those of known Ta'uan representatives, is important to decipher the petrogenetic evolution of this eastern end of the Samoan chain. Despite an enigmatic trace, the Samoan plume resembles other main deep plumes in their seismic anomalies (Ritsema & Allen, 2003).

ACKNOWLEDGMENTS. Particular thanks are due to Leslie Hale for recovering the three basalt samples from the Smithsonian petrology collection and to Dr Sorena Sorensen for authorising their loan and analysis. Support was provided by the Auckland University Research Committee and by a Visiting Fellowship awarded by the Smithsonian Institution to KAR. Thanks are also due to Dr Dietmar Müller, Geology Department, University of Sydney, for providing reconstruction of plate motion tracks in the Samoan region, and to Louise Cotterall, Barry Curham, Svetlana Danilova, Dr Ritchie Sims and John Wilmshurst who assisted with analytical and technical expertise. Dr Ian McDougall, Research School of Earth Sciences, Australian National University, examined thin sections for potential for age dating but considered the rocks unsuitable for accurate K-Ar determination. The script was read by Dr Jane Barron, Sydney. Comments on the script were made by Dr B.J. Keating, School of Ocean and Earth Science and Technology, University of Hawaii, while petrological aspects were reviewed by Dr M.O. Garcia, Dept of Geology and Geophysics, University of Hawaii, Honolulu.

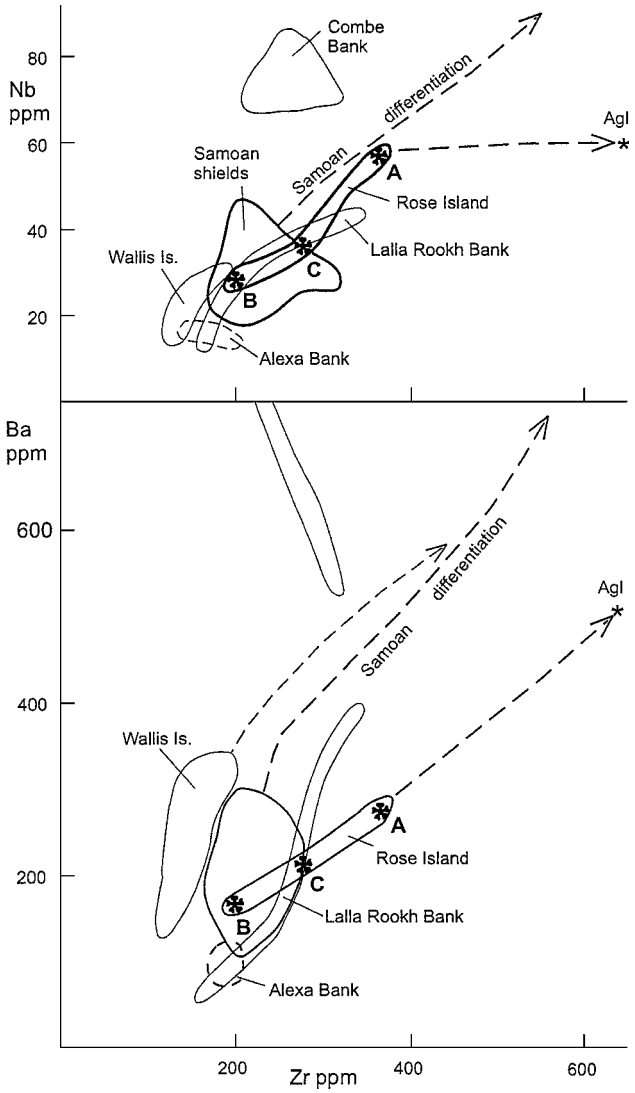

Fig. 8. Nb and Ba related to Zr for Samoan shields, islands and submarine banks. Thick lines: Rose Atoll and Samoan shields; thin lines: Combe Bank, Lalla Rookh bank, Alexa Bank and Wallis Island. Stars: Rose Atoll analyses, this paper. Other data from Natland & Turner (1985), Johnson *et al*. (1986), Price *et al*. (1991).

References

Brothers, R.N., 1959. Petrography. In D. Kear & B.C. Wood. The geology and hydrology of Western Samoa. *New Zealand Geological Survey Bulletin* 63: 38–48.

Buddington, A.F., & D.H. Lindsley, 1964. Iron-titanium oxide minerals and synthetic equivalents. *Journal of Petrology* 5: 310–357.

Carmichael, I.S.E., 1967. The iron-titanium oxides of salic volcanic rocks and their associated ferro-magnesian silicates. *Contributions to Mineralogy and Petrology* 14: 36–64.

Couthouy, J.P., 1842. Remarks upon coral formations in the Pacific; with suggestions as to the causes of their absence in the same parallels of latitude on the coast of South America. *Boston Journal of Natural History* 4: 66–105, 137–162.

Dana, J.D., 1849. *United States Exploring Expedition. During the Years 1838, 1839, 1840, 1841, 1842. Under the Command of Charles Wilkes, U.S.N., v. X. Geology*. C. Sherman, Philadelphia, 309 pp.

Dana, J.D., 1851. On coral reefs and islands. *American Journal of Science and Arts* 61: 357–72, ser. 2, 62: 25–51.

Droop, G.T.R., 1987. A general equation for estimating Fe^{3+} concentrations in ferromagnesian silicates and oxides from microprobe analyses, using stoichiometric criteria. *Mineralogical Magazine* 51: 431–435.

Duncan, R.A., 1985. Radiometric ages from volcanic rocks along the New Hebrides—Samoa lineament. In *Geological Investigations of the Northern Melanesian Borderland*, ed. T.M. Brocker, pp. 67–76. Houston, Texas: Circum-Pacific Council for Energy and Resources.

Farley, K.A., J.H. Natland & H. Craig, 1992. Binary mixing of enriched and undegassed (primitive?) mantle components (He, Sr, Nd, Pb) in Samoan lavas. *Earth and Planetary Science Letters* 111: 183–199.

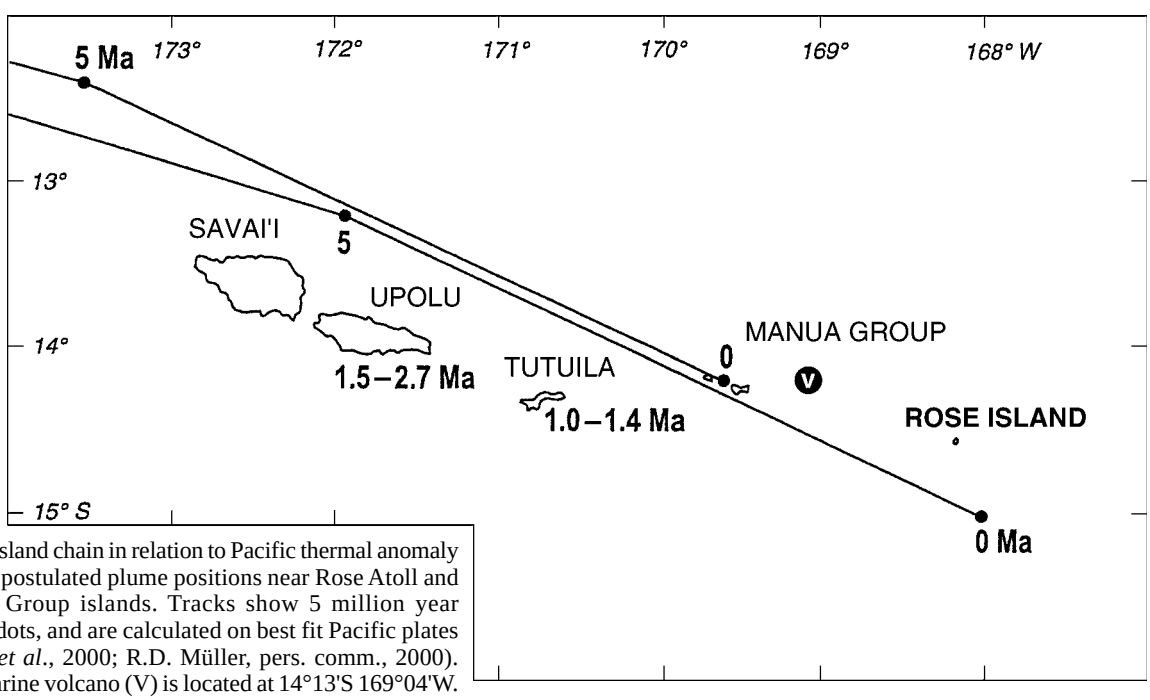

Fig. 9. Samoan Island chain in relation to Pacific thermal anomaly tracks based on postulated plume positions near Rose Atoll and in the Manu'a Group islands. Tracks show 5 million year intervals, solid dots, and are calculated on best fit Pacific plates motion (Gaina *et al*., 2000; R.D. Müller, pers. comm., 2000). Vailulu'u submarine volcano (V) is located at 14°13'S 169°04'W.

Gaina, C., R.D. Müller & S. Cande, 2000. Absolute plate motion, mantle flow and volcanism at the boundary between the Pacific and Indian Ocean mantle domains since 90Ma. In *The History and Dynamics of Global Plate Motions*, ed. M.A. Richards, R.G. Gordon & R.D. van der Hilst, vol. 121, pp. 189–210. American Geophysical Union Monograph.

Garcia, M.O., D.J.P. Foss, H.B. West & J.J. Mahoney, 1995. Geochemical and isotopic evolution of Loihi Volcano, Hawaii. *Journal of Petrology* 36: 1647–1674.

Hart, S.R., H. Staudigel, A.A.P. Koppers, J. Blusztajn, E.T. Baker, R. Workman, M. Jackson, E. Hauri, M. Kurz, K.Sims, D. Fornari, A. Saal & S. Lyons, 2000. Vailulu'u undersea volcano: the new Samoa. *Geochemistry, Geophysics Geosystems Research Letter* 1: 1–13.

Hauri, E.H., N. Shimizu, J.J. Dieu & S.R. Hart, 1993. Evidence for hotspot-related carbonatite metasomatism in the oceanic upper mantle. *Nature* 365: 221–227.

Hawkins Jr., J.W., & J.H. Natland, 1975. Nephelinites and basanites of the Samoan linear volcanic chain: their possible tectonic significance. *Earth and Planetary Science Letters* 24: 427–439.

Hedge, C.E., Z.E. Peterman & W.R. Dickinson, 1972. Petrogenesis of lavas from Western Samoa. *Geological Society of America Bulletin* 83: 2709–2714.

Hieronymous, C.F., & D. Bercovici, 1999. Discrete alternating hotspot islands formed by interaction of magma transport and lithospheric flexure. *Nature* 397: 605–607.

Hoskin, P.W.O., 1998. Minor and trace element analyses of natural zircon ($ZrSiO_4$) by SIMS and laser ablation ICPMS: a consideration and comparison of two broadly competitive techniques. *Journal of Trace Microprobe Techniques* 16: 301–326.

Hubbard, N.J., 1971. Some chemical features of lavas from the Manu'a Islands, Samoa. *Pacific Science* 25(2): 178–187.

Hutchison, C.S., 1974. *Laboratory Handbook of Petrographic Techniques*. New York: John Wiley & Sons.

Johnson, K.T.M., J.M. Stinton & R.C. Price, 1986. Petrology of seamounts northwest of Samoa and their relation to Samoan volcanism. *Bulletin of Volcanology* 48: 225–235.

Kamber, B.S., & K.D. Collerson, 2000. Zr/Nb systematics of ocean island basalts reassessed—the case for binary mixing. *Journal of Petrology* 41: 1007–1021.

Keating, B.H., 1992. The geology of the Samoan Islands. In *Geology and Offshore Mineral Resources of the Central Pacific Basin*, ed. B.H. Keating & B.R. Bolton, vol. 14, pp. 127–178. Circum-Pacific Council for Energy and Mineral Resources Earth Science Series.

Keller, R.A., M.R. Fisk & W.M. White, 2000. Isotopic evidence for Late Cretaceous plume-ridge interaction at the Hawaiian hotspot. *Nature* 405: 673–676.

Larsen, T.B., & D.A. Yuen, 1997. Ultrafast upwelling bursting through the upper mantle. *Earth and Planetary Science Letters* 146: 393–399.

Le Maitre, R.W., 1984. *A Classification of Igneous Rocks and Glossary of Terms*. Oxford: Blackwell, 193 pp.

Macdonald, G.A., 1944. Petrography of the Samoan Islands. *Bulletin of the Geological Society of America* 55: 1333–1362.

Macdonald, G.A., 1968. A contribution to the petrology of Tutuila, American Samoa. *Sonderuck aus der Geologischen Rundschau* 57: 821–837.

McDougall, I., 1985. Age and evolution of the volcanoes of Tutuila, American Samoa. *Pacific Science* 39: 311–320.

Mayor, A.G., 1921. Rose Atoll, American Samoa. *Proceedings of the American Philosophical Society* 60(2): 62–70.

Mayor, A.G., 1924. Rose Atoll, American Samoa. *Carnegie Institution of Washington Publication* 340: 73–79.

Menard, H.W., 1986. Islands. Scientific American, New York. 230p.

Natland, J.H., 1980. The progression of volcanism in the Samoan linear volcanic chain. *American Journal of Science* 280: 709–735.

Natland, J.H., & D.L. Turner, 1985. Age progression and petrological development of Samoan shield volcanoes: evidence from K-Ar ages, lava compositions, and mineral studies. In *Geological Investigations of the Northern Melanesian Borderland*, ed. T.M. Brocher, vol. 3, pp. 139–171. Circum-Pacific Council for the Energy and Mineral Resources Earth Science Series.

Norman, M.D., & M.O. Garcia, 1999. Primitive magmas and source characteristics of the Hawaiian plume: petrology, geochemistry of shield picrites. *Earth and Planetary Science Letters* 168: 27–44.

Parker, R.J., 1994. *Major Element Analysis: Methods and HP-86 Computer Programs*, version 3.0. Department of Geology, University of Auckland Report 3: 1–32.

Pickering, C., 1876. *United States Exploring Expedition. During the Years 1838, 1839, 1840, 1841, 1842 Under the Command of Charles Wilkes, U.S.N. v. XV. The Geographical Distribution of Animals and Plants. Part II, Plants in their Wild State*. Salem, Massachusetts: Naturalists Agency, 524 pp.

Price, R.C., P. Maillet, I. McDougall & J. Dupont, 1991. The geochemistry of basalts from the Wallis Islands, Northern Melanesian Borderland: evidence for a lithospheric origin for Samoan-type basaltic magmas? *Journal of Volcanology and Geothermal Research* 45: 267–288.

Ritsema, J., & R.M. Allen, 2003. The elusive mantle plume. *Earth and Planetary Science Letters* 207: 1–12.

Rodgers, K.A., I. McAllan, C. Cantrell & B. Ponwith, 1993. Rose Atoll: an annotated bibliography. *Technical Reports of the Australian Museum* 9: 1–37.

Sachet, M.-H., 1954. A summary of information on Rose Atoll (Samoa Islands). *Atoll Research Bulletin* 29: 1–25.

Sachet, M.-H., 1955. Pumice and other extraneous volcanic material on coral atolls. *Atoll Research Bulletin* 37: 1–27.

Schultz, L.P., 1940. The Navy surveying expedition to the Phoenix and Samoan Islands. Smithsonian Institution Exploration and Fieldwork in 1939, pp. 45–50.

Setchell, W.A., 1924. American Samoa, part III, vegetation of Rose Atoll. *Carnegie Institution of Washington Publication* 341: 225–261.

Stice, G.D., 1968. Petrography of the Manu'a Islands, Samoa. *Contribution to Mineralogy and Petrology* 19: 343–357.

Sun, S.-s, & W.F. McDonough, 1989. Chemical and isotopic systematics of oceanic basalts: implications for mantle compositions and processes. In *Magmatism in the Ocean Basins*, ed. D.A. Saunders & M.J. Norry, vol. 42, pp. 313–345. Geological Society Special Publication.

Sun, S.-s, W.F. McDonough & A. Ewart, 1989. Four component model for East Australian basalts. In *Intraplate Volcanism in Eastern Australia and New Zealand*, ed. R.W. Johnson, pp. 333–347. Cambridge: Cambridge University Press.

Wells, P.R.A., 1977. Pyroxene thermometry in simple and complex systems. *Contributions to Mineralogy and Petrology* 62: 129–139.

White, W.M., & A.W. Hofmann, 1982. Sr and Nd isotope geochemistry of oceanic basalts and mantle evolution. *Nature* 296: 821–825.

Wilkes, C., 1844. *Narrative of the United States' Exploring Expedition During the Years 1838, 1839, 1840, 1841, 1842*. Vol. 2, xvi. Philadelphia: C. Sherman, 505 pp.

Wood, B.J., & S. Banno, 1973. Garnet-orthopyroxene and orthopyroxene-clinopyroxene relationships in simple and complex systems. *Contributions to Mineralogy and Petrology* 42: 109–121.

Wright, E., & W.M. White, 1987. The origin of Samoa: new evidence from Sr, Nd and Pb isotopes. *Earth and Planetary Science Letters* 81: 151–162.

Manuscript received 13 August 2001, revised 22 August 2002 and accepted 30 August 2002.

Associate Editor: G.D. Edgecombe.